Catalysis Science & Technology

ROYAL SOCIETY OF CHEMISTRY

REVIEW

View Article Online
View Journal | View Issue

Cite this: *Catal. Sci. Technol.*, 2023, **13**, 6342

Methane monooxygenases; physiology, biochemistry and structure

Yasuyoshi Sakai, *[a] Hiroya Yurimoto [a] and Seigo Shima *[b]

Methane-utilizing bacteria (methanotrophs), which inhabit various environments such as wetlands, rice paddies and the surface of aquatic plants are known to convert methane to methanol using methane monooxygenase enzymes (MMOs). There are two distinct types of MMOs: the copper-containing membrane-bound enzyme (pMMO) and the iron-containing soluble enzyme (sMMO). Since MMOs catalyze methane oxidation at ambient temperature and pressure, they are potential biocatalysts for industrial methanol production from methane. Understanding the mechanism of the MMO-catalyzed reaction is crucial to develop a new biocatalyst. The catalytic mechanism of MMO has been extensively studied in aspects of enzyme kinetics, protein structure, spectroscopy, biomimetic chemistry and computation. Based on these studies, the catalytic mechanism of sMMO is relatively well understood, and a rigid catalytic mechanism is proposed. On the other hand, the studies of pMMO are still at their early stages and there are debates as to which of several copper sites are the true active sites. In this review, we describe our current knowledge of MMOs including the metabolism, regulation of expression, their enzymatic properties, and the structural and biochemical features. We summarize recent structural and biochemical studies of pMMO and discuss the future directions to develop efficient and robust biocatalysts.

Received 29th May 2023,
Accepted 28th September 2023

DOI: 10.1039/d3cy00737e

rsc.li/catalysis

1. Introduction

Since the shale gas revolution, interest in using methane, the main component of natural gas, not only as a fuel but also as a carbon source for the production of useful materials has increased worldwide. In addition to being found as a natural resource, methane can be produced from biomass (methane

[a] *Division of Applied Life Sciences, Graduate School of Agriculture, Kyoto University, Kitashirakawa-Oiwake, Sakyo-ku, Kyoto 606-8502, Japan. E-mail: sakai.yasuyoshi.8x@kyoto-u.ac.jp; Fax: +81 75 753 6454; Tel: +81 75 753 6385*
[b] *Max Planck Institute for Terrestrial Microbiology, Karl-von-Frisch-Straße 10, 35043 Marburg, Germany. E-mail: shima@mpi-marburg-mpg.de; Fax: +49 6421 178199; Tel: +49 6421 178100*

Yasuyoshi Sakai

Yasuyoshi Sakai is a Professor at Kyoto University, Japan. He received his Ph.D. degree from Kyoto University, a young scholar fellowship from JSPS, and was appointed as an Assistant Professor in 1988. In 1994, he became an Associate Professor, and a Professor at Kyoto University in 2005 –present. His research has been dedicated to molecular and cell biology and biotechnology of the methylotrophic yeast, in which he revealed the molecular mechanism of methanol-induced gene expression, organelle degradation via autophagy, and established the gene expression system. He received Japan Society for Bioscience, Biotechnology, and Agrochemistry (JSBBA) award in 2022.

Hiroya Yurimoto

Hiroya Yurimoto is an Associate Professor at Kyoto University, Japan. He received his Ph.D. degree from Kyoto University. Then he became an Assistant Professor at Kyoto University in 1996, and an Associate Professor in 2007 –present. His research interests include molecular basis of metabolism, cellular physiology, and gene regulation of C1-microorganisms which can utilize methane and methanol as the sole carbon source, and their application in production of useful chemicals and proteins.

fermentation) or CO_2 (methanation).[1,2] Along with the progress in the technological and conceptional development of "carbon neutral methane" production, there are great expectations for methane as a carbon and energy source in a decarbonized society.[3] In the production of useful compounds from methane, it is desirable to convert it into methanol, which is used as a raw material for various chemical products.[4] However, there are no feasible industrial processes for producing methanol by direct oxidation of methane. At present, methanol is produced through an indirect reaction using synthesis gas (syngas), which contains mainly CO and H_2, produced from natural gas or coal at high temperatures, pressures and energy inputs.[5,6] Therefore, the development of novel catalysts for the direct oxidation of methane to methanol under ambient conditions is highly desirable especially for application in biotechnology.

In nature, there is a group of microorganisms (C_1 microorganisms) that utilize C_1 compounds such as methane and methanol as carbon and energy sources.[7,8] C_1 microorganisms are ubiquitously found in various environments and contribute to drive the global carbon cycle (methane cycle) between the two major greenhouse gases methane and CO_2.[9,10] In the methane cycle, methane is produced by methanogenic archaea in anaerobic environments such as wetlands, paddy fields and the rumen of cattle. The annual emission of methane is estimated to be 560 Tg,[11,12] however, this value may be underestimated because it has recently been reported that methane is produced from methyl radicals generated by the action of reactive oxygen species in the cells of plants and other organisms even in an aerobic environment.[13,14] More than 80% of the methane released into the atmosphere is oxidized by hydroxyl radicals, and most of the rest is consumed by methane-utilizing bacteria (methanotrophs) before being released into the atmosphere.[9] Methane monooxygenases (MMOs) of methanotrophs are responsible for the oxidation of methane to methanol under ambient temperature and pressure.[15–19] Besides MMOs, ammonia monooxygenase and butane monooxygenase have been reported to be able to oxidize methane.[20,21] MMOs are the sole enzymes responsible for the physiological oxidation of methane to methanol and the use of methanotrophs or MMOs has been thought to be promising for direct oxidation of methane to methanol and the production of useful compounds from methane since the 1970s.[22] However, due to problems with the large-scale preparation of MMOs or cells of methanotrophs and the low stability of MMOs, they have not been used in industrial applications yet.

In this review, after overviewing the physiology of methanotrophs and general properties of MMOs, we describe the current understanding of the structural features and reaction mechanisms of pMMO. Finally, attempts to develop efficient and robust biocatalysts for methane oxidation and future perspectives are described.

Seigo Shima

Seigo Shima started his career as a scientist at the Central Research Institute of Electric Power Industry (Japan) in 1985. He received his Ph.D. in 1991 from the University of Tokyo. In 1993, he received a fellowship from Alexander von Humboldt Foundation to study at Philipps-Universität Marburg, Germany. In 1995, he was appointed as a Group Leader at the Department of Biochemistry of Max-Planck-Institute for Terrestrial Microbiology in Marburg. He is currently a department-independent Research Group Reader at Max-Planck-Institute for Terrestrial Microbiology in Marburg. His current research focuses on the catalytic mechanisms of the enzymes involved in methanogenesis.

2. Methanotrophs and methane metabolism

2.1 Physiology and classification of methanotrophs

Methanotrophs inhabit both aerobic and anaerobic environments, but we focus on aerobic methanotrophs in this review. Anaerobic methane oxidation has been described elsewhere.[10,23,24] Fig. 1 summarizes the general methane metabolism in aerobic methanotrophs. The first reaction of methane oxidation in aerobic methanotrophic bacteria is catalyzed by two types of methane monooxygenases, namely a membrane-bound copper-containing particulate methane monooxygenase (pMMO) and a cytosolic soluble methane monooxygenase (sMMO).[25] pMMO is located in the characteristic intracellular membrane structure in most methanotrophic bacteria, but sMMO is found only in the cytosol of some methanotrophic bacteria.[26] Methanol is oxidized to formaldehyde by pyrroloquinoline quinone (PQQ)-dependent methanol dehydrogenases (MDHs).[15] In addition to the conventional calcium-dependent MDH (MxaFI), the lanthanide-dependent MDH (XoxF) has recently emerged as an important enzyme for methanol metabolism in natural environments.[27–29] Formaldehyde is further metabolized by the oxidation pathway to obtain energy and the assimilation pathway to become cellular components. There are two major types of formaldehyde assimilation pathways, the ribulose monophosphate (RuMP) pathway and the serine pathway.[7,15] Some methanotrophs possess the Calvin-Benson-Bassham (CBB) cycle for the fixation of CO_2.[30,31]

Most aerobic methanotrophs belong to the α-Proteobacteria, γ-Proteobacteria and Verrucomicrobia.[32] Classically, the proteobacterial methanotrophs are divided into type I and type II based on their taxonomy at phylum level, and physiological and morphological traits.[7,33] Type I methanotrophs belong to γ-Proteobacteria (families

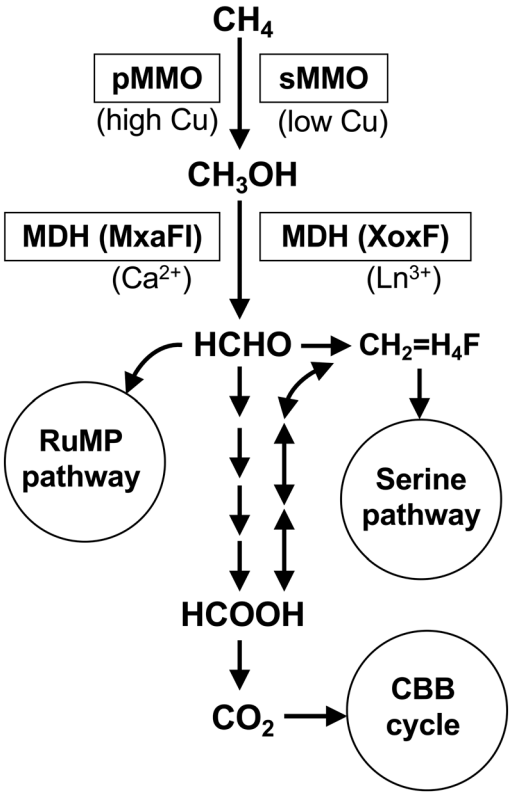

Fig. 1 General methane metabolism in aerobic methanotrophs. pMMO, particulate methane monooxygenase; sMMO, soluble methane monooxygenase; MDH, methanol dehydrogenase; Ln^{3+}, lanthanide ion; $CH_2{=}H_4F$, methylenetetrahydrofolate, RuMP, ribulose monophosphate; CBB, Calvin–Benson–Bassham.

Methylococcaceae and *Methylotermaceae*) and utilize the RuMP pathway for formaldehyde fixation. Type II methanotrophs belong to α-Proteobacteria (families *Methylocystaceae* and *Beijerinckiaceae*) and utilize the serine pathway. A representative methanotroph *Methylococcus capsulatus* Bath is classified as type X because it has both RuMP and serine pathways.[7] *Verrucomicrobia*, which have been discovered relatively recently, are not included in the conventional classification. Verrucomicrobial methanotorphs are extremophiles living in acidic geothermal ecosystems and they possess only pMMO.[34] Very recently, *Candidatus* Mycobacterium methanotorophicum belonging to *Actinobacteria* has been reported to have methanotrophic traits.[35] Methane oxidation in this species is catalyzed by sMMO and formaldehyde fixation by the RuMP pathway.

Almost all methanotrophs are obligate C_1 utilizers, *i.e.*, they utilize only methane or methanol, while some species in the genera *Methylocella*, *Methylocapsa*, *Methylooceanibacter* and *Methylocystis* were found to be facultative methanotrophs that can utilize multi-carbon compounds, such as acetate, ethanol and short-chain alkanes.[32] All known *Methylocella* strains and *Methylooceanibacter methanicus* R-67171 possess only sMMO, whereas other facultative methanotrophs possess only pMMO or both.[32]

2.2 Structure of MMO genes and their regulation

pMMO and sMMO have completely different properties with respect to substrate specificity, metal ions involved, and protein structure. pMMO has a trimer of heterotrimers consisting of three subunits, PmoA, PmoB, and PmoC, encoded by the *pmoCAB* gene operon (Fig. 2).[36,37] The structure of pMMO is described in the section 3.4.[37] Some methanotrophs of the *Methylocystaceae* family produce methanobactin, a peptide with high affinity to Cu(I) ion which contributes copper ion trafficking into the bacterial cells.[15,38] Another example of the copper collection is a surface-bound protein (MopE) and a secreted form of it (MopE*) in *M. capsulatus*.[39]

sMMO has a binuclear iron-active center, and recently, the structure of important chemical species involved in the reaction have also been elucidated.[18,40] sMMO consists of a hydroxylase (MMOH) that catalyzes methane hydroxylation, a regulatory protein MMOB, and a reductase MMOR. MMOH is a dimer of heterotrimers encoded by the *mmoXYZ* genes (Fig. 2).[18,36] The α subunit has a binuclear iron active center, where the activation of molecular oxygen and the oxidation of methane take place. MMOR, encoded by the *mmoC* gene, contains FAD and an iron–sulfur cluster (2Fe-2S). It accepts electrons from NADH, and reduces the active center of the α subunit. MMOB, which is encoded by the *mmoB* gene, regulates the transfer of electrons.[18] Furthermore, the *mmo* gene cluster contains the *mmoG* gene, which encodes a chaperone-like protein that mediates protein folding, and the *mmoD* and *mmoR* genes, which are thought to be involved in the regulation of gene expression.[41,42]

In methanotrophs, which have both pMMO and sMMO, the production of pMMO is up-regulated and sMMO is down-regulated at the transcriptional level under copper-ion rich conditions.[36] sMMO is expressed when the copper/biomass ratio is low and down-regulated in high copper conditions. This type of regulation is known as the copper switch. The copper switch has been well investigated at the molecular level using a representative methanotroph, *Methylosinus tricosporium* Ob3B. Several genes, *rpoN*, *mmoR*, *mmoG* and *mmoD*, were found to play key roles in the regulation of expression of the *mmo* operon.[41,42] Methanobactin may also contribute to the Cu sensing mechanism and the regulatory

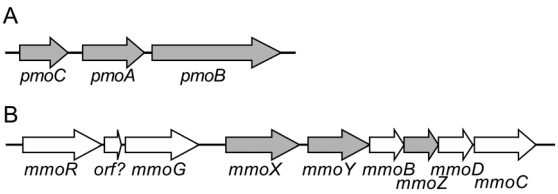

Fig. 2 Gene organization of pMMO- and sMMO-encoding operons of *M. trichosporium* OB3b. (A) The pMMO operon. The *pmoA*, *pmoB*, and *pmoC* encode three subunits of pMMO, PmoA (24 kDa), PmoB (47 kDa), and PmoC (22 kDa). (B) The sMMO operon. The *mmoX*, *mmoY*, and *mmoZ* encode three subunits of MMOH, α (60 kDa), β (45 kDa), and γ (19 kDa).

genes associated with methanobactin, *mbnI* and *mbnR*, may play a role in the copper switch.[15]

sMMO belongs to a large enzyme family of soluble diiron monooxygenases (SDIMOs), which catalyze the oxidation of a wide range of hydrocarbons including short-chain alkanes, alkenes, and aromatic compounds.[43,44] SDIMOs consist of six groups based on DNA sequence, gene organization, subunit composition, and substrate specificity. sMMOs are part of group 3. The facultative methanotrophs belonging to *Methylocella* sp. have a group 5 SDIMO, propane monooxygenase (PrMO), in addition to sMMO, and can utilize propane as a carbon source.[44,45] In *Methylocella silvestris*, the sMMO genes but not the PrMO genes are expressed during growth on methane, whereas both genes are expressed during growth on propane.[45]

3. Biochemistry of particulate methane monooxygenase

The nature and the catalytic mechanism of sMMO have been extensively studied using biochemistry, spectroscopy, X-ray crystallography and cryo-electron microscopy (cryo-EM), and a plausible catalytic mechanism has been proposed.[40] The structure, function and catalytic mechanism of sMMO, has been reviewed elsewhere.[18,19,25,46] On the contrary, despite the fact that many active researches have been carried out, the nature of the active site structure and the catalytic mechanism of pMMO are still controversial, although pMMO is a chemically and biotechnologically very important enzyme.[16,17] In this section, we shortly review some critical experimental results about pMMO to understand the current status of the study of this enzyme for further development.

3.1 Solubilization and purification of pMMO

pMMO is located in the inner cell membrane of methanotrophic bacteria[47] and is fractionated into the particulate fraction of the cell extract (Table 1). The occupancy of pMMO in the membrane protein fraction is very high, accounting for ~80% of the membrane proteins and ~20% of the total proteins in the cells.[47,48] The presence of such a large amount of pMMO in the cells implies a relatively low specific activity of this enzyme compared to the other metabolic enzymes. Comparison of the washed membrane fractions obtained from *M. capsulatus* showed that the copper-enriched cells contained significantly more copper ions.[49]

The activity of pMMO is unstable, and upon when cells are disrupted, much of the methane monooxygenase activity found in the whole cells disappears (Table 1). Nevertheless, it is possible to purify pMMO by tracking the residual enzymatic activity. To purify the membrane protein from the particulate fraction, the membrane protein is solubilized by using detergents. Again, much activity is lost in the solubilization step. The Dalton group reported solubilization of pMMO by using dodecyl-β-D-maltoside as a detergent, which abolished the enzyme activity, but the addition of egg or soybean lipids reactivated the enzyme,[50] which suggests that lipids are required to maintain the active structure of pMMO. This finding is supported by reports on the effect of

Table 1 Character of purified pMMO

	Specific activity (mU mg^{-1})						
	Whole cell	Membrane fraction	Solubilized	Purified	Metal ions/heterotrimer	EPR signals	References
Methylococcus capsulatus Bath[a]	60.5 (273 000)[b]	10.4 (28 000)[b]	9.86 (19 000)[b]	11.1 (11 000)[b]	14.6 ± 1.9 Cu 2.5 ± 0.7 Fe	Type 2 Cu High-spin Fe Broad low-field	Zahn *et al.* 1996 (ref. 55)
Methylococcus capsulatus Bath[c]		9.66–12.5		2.6–5.1	12.4–15 Cu Fe, not detected	Type 2 Cu Broad-isotropic Cu	Nguyen *et al.*1998 (ref. 54)
Methylococcus capsulatus Bath[d]		21 (NADH) 16 (duroquinol)	n.d. (NADH) 3.9 (duroquinol)	n.d. (NADH) 17.7 (duroquinol)	4.8 ± 0.8 Cu[e] 1.5 ± 0.7 Fe[e]	Type 2 Cu	Lieberman *et al.* 2003 (ref. 58)
Methylosinus trichosporium OB3b (30 °C)[f]		2.3 (668)[b]	0.24 (35)[b]	0.47 (5.7)[b]	12.8 Cu 0.9 Fe	Type 2 Cu High-spin Fe	Takeguchi *et al.* 1998 (ref. 57)
Methylosinus trichosporium OB3b[g]		2.2 (NADH) 3.8 (duroquinol)		n.d. (NADH) 3.3 (duroquinol)	2 Cu	Type 2 Cu High-spin Fe	Miyaji *et al.* 2002 (ref. 56)
Methylocystis sp. M[h]	~500 (CH_4)	~250 (methane) ~70 (propene)	Not reported	0–10 (methane) 05 (propene)	1–3 Cu 0.08–1 Fe	Not tested	Gvozdev *et al.* 2006 (ref. 60)

[a] The enzyme assay was performed at 45 °C by measuring propylene epoxidation with duroquinol, in which the whole cell activity was measured using formate as the reductant. [b] Total activity. [c] The enzyme assay was performed at 45 °C using propane, butane oxidation or propene epoxidation. NADH was used as the reductant. [d] The enzyme assay was performed at 45 °C by measuring epoxidation of propylene with NADH. [e] The metal was calculated per 200 kDa dimer of heterotrimer. [f] The enzyme assay was performed at 30 °C by measuring propene epoxidation with duroquinol. [g] The enzyme assay was performed by measuring propylene epoxidation with NADH or duroquinol. [h] The enzyme assay was performed by measuring methane oxidation or propene epoxidation with duroquinol.

lipid structures (bicelles and nanodiscs) on the pMMO activity (see below).[51–54] However, in most of the reports, active pMMO was purified from the detergent-solubilized fraction by column chromatography using detergent-containing buffer solutions.[55–58]

Tonge *et al.* first purified pMMO from *M. trichosporium OB3b*.[59] They followed the enzymatic activity by measuring the conversion of methane to methanol using ascorbic acid as an electron donor. However, the size of the proteins in the purified fraction differed from the standard protein composition of the subsequently purified pMMO. Zahn and DiSpirito purified pMMO, which has a typical pMMO subunit composition, from *M. capsulatus* Bath, in which the total activity from the whole cells was reduced to 10% by disruption of the cells, and subsequent solubilization resulted in a 67% yield.[55] In total, 4% of the pMMO activity from whole cells was obtained in the purified fraction (Table 1). The specific activity of the purified enzyme was 11 mU mg^{-1}, where one U of enzyme is defined as the activity of catalyzing 1 μmol propylene epoxidation per minute with duroquinol as the reductant.[55] Later, Nguyen *et al.* also reported the purification of pMMO from the same organism, where the specific activity of the purified enzyme was 2.6–5.1 mU mg^{-1}.[54] In addition, Liebermann *et al.* reported a slightly higher activity (17.7 mU mg^{-1}) of the purified enzyme from the same organism.[58] In the case of *Methylocystis* sp. M, 50% of the cellular activity was recovered in the membrane fraction, but less than a few percent of the enzyme activity was detected in the purified enzyme.[60] In the case of *M. trichosporium* OB3b, less than 1% of the activity in the membrane fraction was obtained in the purified fraction, in which the final specific activity was 0.5 mU mg^{-1}.[57] Thus, the yield of isolating pMMO activity from cells is generally very low.

Purified pMMO contains copper ions. However, the amount of copper ions in purified pMMO preparations varies (Table 1). Partial removal of the copper ions by EDTA from purified pMMO from *M. trichosporium* OB3b and *M. capsulatus* Bath decreased the enzyme activity and addition of external copper ions reactivated the enzyme.[61–64] A stimulating effect of addition of copper ions on the pMMO activity of the membrane fraction of *M. capsulatus* Bath was reported, in which the Cu(II) electron paramagnetic resonance (EPR) signal increased with MMO activity.[49,65] Thus, the copper ions are critical for the enzymatic activity of pMMO but they are only loosely bound to the protein, and addition of external copper ions can restore the copper site by diffusing into the binding sites. This finding suggests that the loosely bound copper ions in pMMO should be simple copper ions complexed by amino-acid residues rather than complicated metal complexes. In addition, these observations suggest that the copper active site is likely exposed to the solvent and not deeply embedded in the protein core. Interestingly, copper ions are also inhibitory at higher concentrations,[49] suggesting that external copper ions may bind to the active site copper complex. The reversible binding of copper ions to the pMMO provides some clues to the character of the active site; however, this property makes it difficult to determine the number and character of copper ions in purified pMMO.

3.2 pMMO activity assay

pMMO oxidizes a wide range of substrates including alkanes and alkenes.[66] Most of the purification work used propylene epoxidation activity rather than methane oxidation because of the difficulty of detecting the latter reaction. As summarized by Koo *et al.*, many of the purified pMMOs show no enzymatic activity against methane unless reconstituted with lipids.[53] The use of the propylene epoxidation assay is based on the hypothesis that methane oxidation and propylene epoxidation are catalyzed by the same active site. If the enzymatic activity of the purified pMMO preparations has not been determined by the methane oxidation assay, the data should be interpreted with caution.

The direct physiological reductant of the pMMO reaction has been proposed to be the reduced form of quinone or NADH. NADH is the physiological electron donor of sMMO and this electron carrier should be involved in the reaction sequence of metabolism involving the pMMO reaction. In fact, membrane-fractions and some purified pMMO preparations use NADH as an electron donor (Table 1). Quinol is reproduced from quinone by membrane enzymes involved in the respiratory chain. Choi *et al.* purified pMMO from *M. capsulatus* Bath as a complex with type 2 NADH: quinone oxidoreductase.[67] This finding supports the hypothesis that quinone is the direct electron carrier for pMMO. However, it was recently shown by cryo-electron tomography that pMMO molecules themselves form higher-order hexagonal arrays in intact cells,[47] suggesting that pMMO and type 2 NADH:quinone oxidoreductase do not always form a tight complex. Most enzyme assays use a quinonol analog, duroquinol, but some purified pMMO show activity when using NADH,[17] which may be mediated by minute amounts of contaminating type 2 NADH:quinone oxidoreductase.[67]

The use of duroquinol as a reductant in the pMMO reaction was introduced by Shiemke *et al.*[68] This compound is an analogous to biological quinoles but with relatively higher solubility in water-based solutions. The redox potential at pH 7 of duroquinol is +7 mV.[69] Duroquinol is a useful compound for detecting pMMO activity; however, great care must be taken when measuring the enzyme preparation with very low pMMO activity. This is because duroquinol reduces O_2 to form H_2O_2,[70] which becomes a hydroxy radical and oxidizes methane.[71] The pMMO preparation contains a certain amount of copper ions, which accelerate the formation of H_2O_2 and the hydroxy radical.[72,73] Therefore, the pMMO activity measured in the presence of duroquinol and copper ions shows a certain background of the non-specific methanol-producing activity. This background activity can mislead the enzymatic activity of the pMMO.

To confirm non-enzymatic methane oxidation in the presence of duroquinol or H_2O_2, we tested the methane

oxidation using [^{13}C]-methane as a substrate. We added 5 mg of duroquinol or 500 mM of H_2O_2 in 250 μl of phosphate-buffered saline pH 7.0 in a 7.7 ml sealed vial, into which 5 mL of [^{13}C]-methane was injected, and incubated the vial at 28 °C or 35 °C for 4 h. We quantified the amount of [^{13}C]-methanol in the reaction mixture by gas-chromatography coupled to mass-spectrometry (GC/MS) analysis. The reaction rates at 35 °C were estimated to be 3.0×10^{-2} μM min^{-1} (duroquinol) and 6.8×10^{-2} μM min^{-1} (H_2O_2). These rates are comparable to the production of methanol by the heterologously-produced soluble-domain of the PmoB subunit (spmoB) reported by Ross *et al.* (approximately 10 μM methanol production for a 1 h reaction at 45 °C).[71] Thus, we confirmed that duroquinol and H_2O_2 caused non-enzymatic oxidation of methane at ambient temperature in the absence of a biological or artificial catalyst.

3.3 Inhibitors of pMMO

The inhibitors of pMMO can be classified into three types; (i) analogs of the substrate or product of pMMO: acetylene,[55,74,75] duroquinol,[76] duroquinone,[77] and oxygen[54,55] and H_2O_2;[78] (ii) chelating or metal-binding reagents: azide,[55] cyanide,[55,68,79] EDTA,[68] and nitrite;[71] and (iii) metal ions: copper,[49] zinc.[80] Acetylene and acetylenic compounds react with O_2 and reducing equivalents and irreversibly inhibit pMMO by binding the reaction product to the protein.[75] Isotope labeling with [^{14}C]-acetylene showed that the reaction product localized to the 26–27 kDa band on SDS-PAGE, the size of which corresponds to the PmoA subunit of pMMO.[55,75] On the other hand, Pham *et al.* reported that the acetylene-reaction product is bound to the residue of PmoC.[74] Because the reaction product of acetylene, ketene, can move from the active site to another position in the protein, exact localization of the active site is not easy to determine.[74]

The inhibitory effect of chelating or metal-binding inhibitors suggest that the active site of pMMO is composed of metal ions. Treatment with cyanide or EDTA partially removed copper ions from pMMO and decreased the enzyme activity,[61–64] indicating that the copper active site is located in the hydrophilic region of pMMO. Zinc is found in the crystal structure when zinc compounds are present in the crystallization solution. The zinc ion is located at the probable copper binding site; therefore, zinc could inhibit the MMO activity by displacing the copper. The zinc-substituted metal-binding site is identified in the Cu_C site of the PmoC subunit (see below), which suggests that the Cu_C site may be the active site of pMMO.[71,80] Inhibition by copper ions suggests that external copper ions may interact with the endogenous copper site, which could form an artificial multinuclear copper cluster. Oxygen affects the activity and oxidation states of pMMO; therefore, most of purification experiments were performed under anoxic conditions.[54,55,61,76]

3.4 Protein structure of pMMO

To discuss the structure and function of the metal centers of pMMO, it is essential to have three-dimensional coordination information. The first protein crystal structure was obtained by the Rosenzweig group using pMMO purified from *M. capsulatus* Bath.[37] The 2.8 Å crystal structure showed a conformation of a trimer of the heterotrimer composed of the 24 kDa PmoA, 47 kDa PmoB, and 22 kDa PmoC (Fig. 3). The PmoA and PmoC subunits are mainly composed of transmembrane helices, which is typical for membrane anchoring proteins. PmoB is mainly located in the cytosolic region and is anchored to the membrane by a hydrophobic domain. There are electron densities corresponding to a mononuclear metal site (Cu_A) and a dinuclear metal site (Cu_B) in PmoB, and a mononuclear metal site in PmoC. X-ray anomalous Fourier maps indicated that the metals at the metal binding sites are copper in PmoB and zinc in PmoC. The zinc-binding site in PmoC could be a site for the copper-binding site in the native form of the enzyme; therefore, this metal site is referred to as the Cu_C site.[37] A zinc ion could be incorporated from the crystallization solution and replaced by the native copper ion.[79–81] Analysis of the purified pMMO indicated the presence of 2 to 15 copper ions and 2 iron ions, but no further binding sites for copper and iron ions were detected in the X-ray crystal structure.[37]

In addition to pMMO from *M. capsulatus* Bath, pMMOs from *M. trichosporium* OB3b,[81] *Methylocystis* sp. M,[79] *Methylocystis* sp. Rockwell,[80] and *Methylomicrobium alcaliphilum* 20Z[51] were analyzed by X-ray crystallography. The metal-binding sites of the pMMO structures found in pMMO from *M. capsulatus* Bath are not fully conserved among the different pMMOs (Table 2). The Cu_B site in PmoB of the pMMO structure in *M. alcaliphilum* 20Z and *Methylocystis* sp. Rockwell was modeled as a mononuclear copper site, and that of *Methylocystis* sp. M was modeled as a mixture of mononuclear and dinuclear copper sites (Fig. 3D and E). The Cu_A mononuclear copper site was not reproduced in other crystal structures of pMMO (Table 2), although the density was observed in the cryo-EM structures.[53,82] At the Cu_C mononuclear metal site of PmoC, a copper ion was identified in the structure of *M. trichosporium* OB3b and *Methylocystis* sp. Rockwell, and zinc was observed in the structure from *Methylocystis* sp. M. In the crystal structure of pMMO from *M. alcaliphilum* 20Z, 60% of the structure of PmoC was disordered and the Cu_C metal site was not observed.[51] The purified samples for crystallization show no or very low activity, which is one of the reason for the difficulty in studying the structure–function relationship of the metal site.[53]

To overcome the instability of pMMO, the Rosenzweig group reported the stabilization of the purified pMMO by reconstitution of a solubilized membrane protein in a lipidic environment using bicelles and nanodiscs, and successfully increased the specific activity of the pMMO preparation.[51,52]

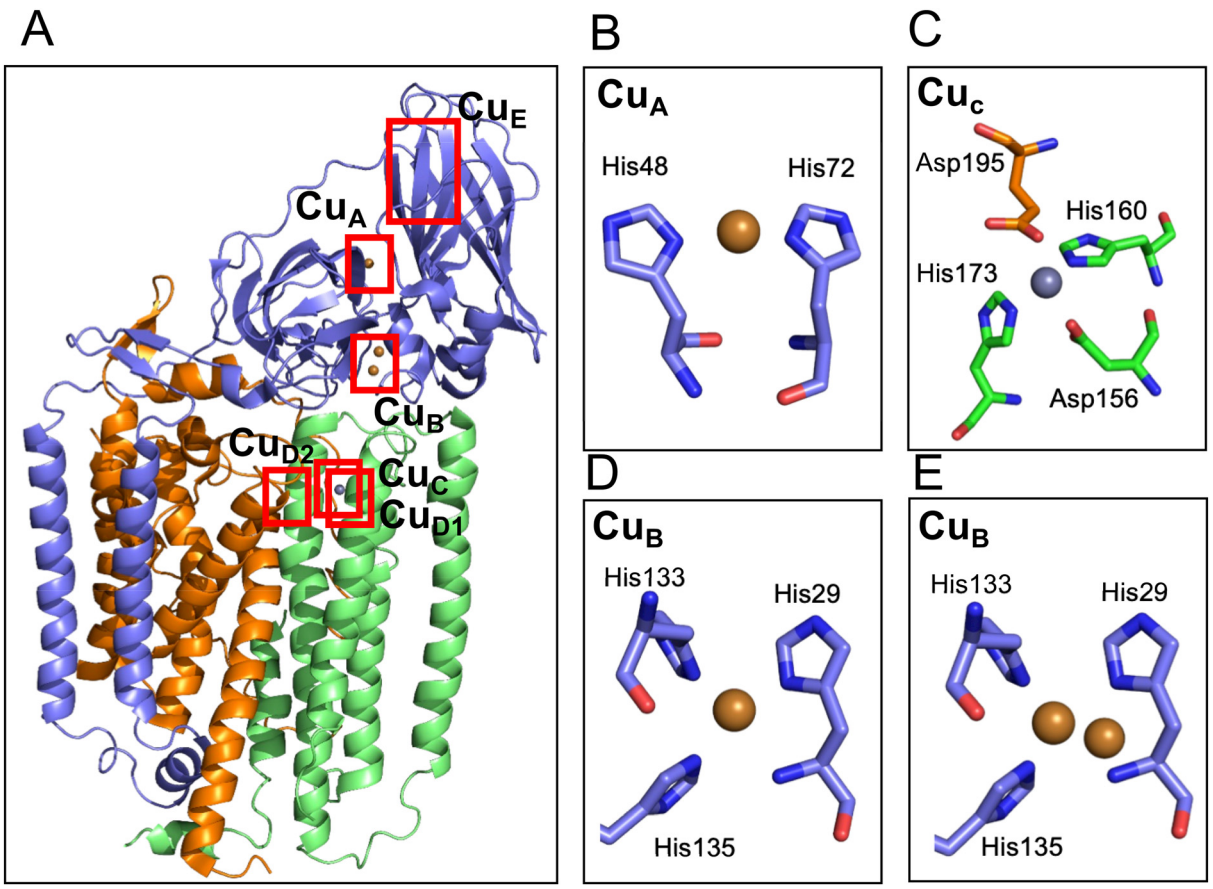

Fig. 3 Cartoon model of the structure of pMMO and the metal sites. (A) Overall structure of pMMO from *M. capsulatus* in heterotrimer (PDB code 1YEW). The cartoon models of the PmoA, PmoB, and PmoC are shown in orange, blue, and green, respectively. The modeled copper and zinc ions are shown as brown and gray spheres, respectively. The ligand structure of Cu_A, Cu_C and two types of Cu_B are shown in the panels B–E. The Cu_E site was modeled only in one of the cryo-electron microscopy structure (Table 2) but not detected in the crystal structure; therefore, the CuE site metals are not depicted in this panel. (B) Cu_A site of pMMO from *M. capsulatus* (PDB code 1YEW). (C) Cu_C site of pMMO from *M. capsulatus* (1YEW). Glu195 is tentatively assigned to bind 2.9 Å away from the Zn site. (D and E) Mononuclear (D) and dinuclear (E) models of the Cu_B site in pMMO from *Methylocystis* sp. M (PDB code 3RFR).

The active reconstituted pMMO in lipid nanodiscs was used for the structural analysis by cryo-EM.[53] As shown in Table 2, the 2.14–2.46 Å cryo-EM structure of the nanodisc-stabilized pMMO from *M. capsulatus* Bath revealed the presence of a new metal site in PmoC, which is proposed to be a mononuclear copper site. We refer to this metal site as Cu_{D1} to distinguish it from a copper D site in PmoA proposed by the Chan group, which is referred to as Cu_{D2} in this review. The protein region at the Cu_{D1} site in PmoC was stabilized by embedding into lipid nanodiscs. The authors proposed that the Cu_{D1} site is the actual methane oxidation active site, which was not visible in the structural analysis of inactive pMMO without stabilization by lipids. The Chan group also reported a 2.5 Å cryo-EM structure of pMMO from *M. capsulatus* Bath, which was solubilized using the detergent *n*-dodecyl-β-D-maltoside.[82] In the cryo-EM density, they modeled several copper ions at the Cu_{D2} site in PmoA and at the Cu_E sites in PmoB (Table 2). In the detergent-solubilized pMMO structure, the Cu_{D1} site was not observed. On the contrary, the Cu_{D2} and Cu_E sites were not observed in the nanodisc-stabilized structure. The quality of the cryo-EM density maps appears to be too low to be used for the discussion of the metal ligand. The presence of the metal ions at the sites must be confirmed by anomalous scattering of the crystal structure and/or careful X-ray absorption spectroscopy (XAS) analysis combined with mutation analysis.

3.5 Copper complex structures based on spectroscopy analyses

3.5.1 Trinuclear copper center. The trinuclear copper center of pMMO was proposed by the Chan group. The EPR spectroscopic analysis of the membrane fraction and purified pMMO revealed the presence of a type 2 copper and a broad isotropic signal. The isotropic signal was interpreted as the presence of the trinuclear copper cluster in pMMO.[49,54] Nguyen *et al.* proposed that the pMMO preparation contains 15 copper ions as five trinuclear copper clusters.[54] The Chan group has also provided experimental results supporting the

Table 2 Character of the partially conserved active-site metals in the pMMO structures

		Modeled metals in the structure of the pMMO subunits and the coordinating residues						
		PmoB	PmoB	PmoC	PmoC	PmoA	PmoB	
Microorganism	Resolution	Cu_A	Cu_B	Cu_C	Cu_{D1}	Cu_{D2}	Cu_E	Ref.
Crystal structure								
Methylococcus capsulatus Bath (1YEW)	2.8 Å	Cu $H_{48}H_{72}$	Cu–Cu (2.57 Å)[a] $H_{33}H_{137}H_{139}$	Zn $D_{156}H_{160}H_{173}E_{A195}$	No metal	No metal	No metal	Lieberman *et al.* 2005 (ref. 37)
Methylosinus trichosporium OB3b (3CHX)	3.9 Å	No metal	Cu–Cu (2.52 Å)[a] $H_{40}H_{144}H_{146}$	Cu $D_{129}H_{133}H_{146}E_{200}$	No metal	No metal	No metal	Hakemian *et al.* 2008 (ref. 81)
Methylocystis sp. M (3RFR)	2.68 Å	No metal	Cu–Cu or Cu[b] $H_{29}H_{133}H_{135}$ (2.52–2.64 Å)[a]	Zn $D_{129}H_{133}E_{146}$	No metal	No metal	No metal	Smith *et al.* 2011 (ref. 79)
Methylocystis sp. Rockwell (4PHZ)	2.59 Å	No metal	Cu $H_{29}H_{133}H_{135}$ (2.48 Å)[c]	Cu $D_{129}H_{133}H_{146}$	No metal	No metal	No metal	Sirajuddin *et al.* 2014 (ref. 80)
Methylomicrobium alcaliphilum 20Z (6CXH)	2.7 Å	No metal	Cu $H_{33}H_{137}H_{139}$	No metal[d]	No metal	No metal	No metal	Ro *et al.* 2018 (ref. 51)
Cryo-EM structure								
Methylococcus capsulatus Bath (7EV9)	2.6 Å	Cu $H_{48}H_{72}$	Cu–Cu $H_{33}H_{137}H_{139}$	No metal	No metal	Cu–Cu[e] $H_{38}M_{42}E_{100}$	Cu–Cu $T_{281}N_{306}D_{395}$ Cu[f] E_{316}	Chang *et al.* 2021 (ref. 82)
Methylococcus capuslatus Bath (7S4H)	2.14 Å	Cu $H_{48}H_{72}$	Cu $H_{33}H_{137}H_{139}$	No metal	Cu $N_{227}H_{231}H_{245}$	No metal	No metal	Koo *et al.* 2022 (ref. 53)

[a] Distance between two Cu ions by EXAFS measurement. [b] A Cu–Cu site is modeled in one of three pmoB subunits, in which the other two PmoB subunits were modeled with a single copper ion. [c] The crystal structure showed single a Cu ion but EXAFS showed a Cu–Cu cluster at a distance of 2.48 Å. [d] Most of the PmoC structure is disordered. [e] The methyl carbon of Met_{42} is modeled to coordinate to a Cu ion in the distance of 1.9 Å. [f] The modeled mononuclear Cu is coordinated only to a single E_{316}, in which the other proposed coordination residues are too distant to ligate; Tyr330 (3.2 Å from the modeled Cu), Arg323 (3.6 Å) and Arg400 (4.0 Å).[82]

presence of the trinuclear copper site, such as theoretical calculation,[83,84] potentiometric titrations[85] and the synthesis of trinuclear copper complexes that catalyze H_2O_2 or O_2 activation and hydrocarbon oxidation.[86–90]

However, the majority of experimental results contradict the hypothesis of the presence of a trinuclear copper site. All structural analyses do not show the presence of the trinuclear copper center (see Table 2). In addition to the data of purified pMMO shown in Table 1, the EPR studies on the samples of *M. capsulatus*,[71,91,92] *M. trichosporium* OB3b,[81] *Methylocystis* sp. M,[79,80] *M. alcaliphilum* 20Z,[51] *Methylomicrobium album* BG8,[93,94] did not show the presence of the trinuclear copper center. Takeguchi *et al.* discussed an EPR signal attributable to the trinuclear clusters in the purified pMMO from the *M. trichosporium* OB3b fraction,[57] but in a later study, the same group concluded the absence of such an EPR signal using pMMO from the same organism with an improved purification method.[56]

3.5.2 Dinuclear copper center. Once a dinuclear copper cluster was modeled in the crystal structure of pMMO,[37] extended X-ray absorption fine structure (EXAFS) analysis of pMMO from several organisms was performed extensively in parallel with the crystal structure analysis and showed the presence of the dinuclear copper site.[37,51,79–81] Exceptionally, the EXAFS data of the bicelles-stabilized pMMO from *M. alcaliphilum* 20Z showed the presence of only mononuclear copper site according to its crystal structure.[51] Notably, pMMO from anaerobic methanotrophic bacteria belonging to *Verrucomicrobia* does not contain the Cu_B-ligating amino acids,[34] which suggests that the possible dinuclear Cu_B site of the PmoB subunit is not the universal active site of pMMO.[71]

3.5.3 Mononuclear copper center. Recent studies indicated that pMMO contains only mononuclear sites.[71,95,96] Ross *et al.* reported the spectroscopic analysis of pMMO in whole cells of *M. capsulatus* to avoid disturbance of the copper content during the extraction and purification of the pMMO samples.[71] In the study, the copper ions and nitrogen atoms were enriched with ^{63}Cu and ^{15}N isotopes, respectively. The whole cell samples showed a type 2 Cu EPR signal with four N equatorial ligands. Electron nuclear double resonance (ENDOR) spectroscopy detected a copper ion ligated with four ^{15}N and weakly coupled resonances from uncoordinated ^{15}N of histidyl imidazoles bound to Cu(II), in which an amino group coordinated to Cu was also detected. The EPR and ENDOR data indicated the Cu_B site as a mononuclear copper site although it was previously modeled as a dinuclear copper site. These data indicate that pMMO contains two monocopper sites at the Cu_C site identified in PmoC and at the Cu_B site in PmoB. When pMMO was inhibited by nitrite, the signal of the Cu_C site changed, which suggested that the Cu_C mononuclear copper site was responsible for the activity.[71] These spectroscopic data were also confirmed using the pMMO preparations from *Methylocystis* sp. Rockwell.[96]

The Holmes group reported that the Cu_C site of an alkane monooxygenase (a pMMO homolog) is absolutely essential for the activity by mutational studies, although the Cu_B site plays a role in supporting the pMMO activity.[97] Thus, these experiments indicated that the mononuclear Cu_C site located in the PmoC subunit is essential for methane oxidation. However, the Rosenzweig group later reported the cryo-EM structure of pMMO from *M. capsulatus* Bath stabilized by embedding into nanodiscs, which revealed an additional copper site ligated with two histidine residues.[53] This novel copper site was named as to Cu_D by Koo *et al.*,[53] which is referred as Cu_{D1} in this review to distinguish it from the above-mentioned trinuclear copper site predicted by the Chan group.[85] The Cu_{D1} site is located close to the Cu_C site. Notably, the copper ion at the Cu_C site was not observed in the cryo-EM structure; therefore, the authors predicted that the Cu_{D1} site might be the copper site spectroscopically observed in the previous spectroscopic analysis.[71]

3.6 Oxidation states of the copper sites

Most of the EPR analysis of the pMMO samples indicated the presence of Cu(II) sites (Table 1). The Cu(II) signal decreased upon reduction with dithionite, indicating that the copper site is redox active and reduced to Cu(I).[49,54,58,92] X-ray absorption near edge (XANE) analysis indicates that the copper in purified pMMO is a mixture of Cu(I) and Cu(II).[37,51,79,81] However, recent work by the DeBeer group pointed out that X-ray beam causes reduction of the copper sites.[98] To minimize the radiation effects, the analyses were performed with lower intensity beam and the authors concluded that most of the copper ion species in pMMO are Cu(II) and the copper sites in pMMO are only mononuclear. The effect of background copper ions is one reason for the misinterpretation of the previous EXAFS data that led to modeling dinuclear copper sites.[98]

3.7 Characterization of the engineered PmoB subunit

The crystal structure of pMMO from *M. capsulatus* Bath indicated that the cytosolic subunit PmoB contains a mononuclear Cu_A and dinuclear Cu_B copper site.[37] A genetically engineered PmoB subunit (spmoB) was heterologously produced in *E. coli*. The hydrophobic membrane-anchoring domain of PmoB was genetically removed in the artificial spmoB protein by conjugation of the soluble regions with a peptide linker.[99] Reconstitution of soluble spmoB from the inclusion bodies in the presence of copper ions produced an active form of psmoB, which exhibited methane mooxygenase activity; epoxidation of propylene to propylene oxide and oxidation of methane to methanol. Mutation of possible copper-binding residues at the Cu_B abolished the enzyme activity but mutation of the residues at the Cu_A site left some residual activity. The authors concluded that the Cu_B site is crucial for the methane monooxygenase activity of this protein.[99] In the same report, EXAFS revealed the coordination structure of the copper site of spmoB, which is similar to that in pMMO.

O_2 or H_2O_2 reacts with the reduced form of pMMO and spomB to change the UV-visible spectrum of pMMO, but the mutants lacking the CuB site did not show the reaction, indicating that the PmoB subunit is responsible for the reaction with the oxidants.[100] In addition, the oxidation states of the copper center of spmoB were studied using quantitative EPR analysis.[101] Kim *et al.* constructed a fusion protein of a PmoB soluble fragment conjugated to ferritin, which increased the solubility of the PmoB fragment.[102] The engineered PmoB fusion protein exhibited methane monooxygenase activity, supporting the previous spmoB studies.[102]

Later, however, an improved form of spmoB was constructed that had increased solubility by conjugating soluble protein regions to spmoB.[16,71] The new form of spmoB does not catalyze the methane monooxygenase activity. Based on these results, the authors discussed that the observed methane monooxygenase activity of the original spmoB in Balasubramanian *et al.*[99] is a background reaction dependent on duroquinol.[71] However, if the observed methane monooxygenase activity is due to a non-enzymatic reaction, then the results of the mutation experiments at the Cu_B ligation site in the previously reported spmoB are contradictry.[99] Even if the PmoB analogues cannot directly catalyze the methane monooxygenase activity, it cannot be excluded that under certain conditions, spomB catalyzes the formation of the reactive oxygen species, that in turn mediate the oxidation of methane to methanol.

Chan *et al.* reported the construction of an engineered PmoB conjugated with a maltose-binding protein.[103] This engineered protein did not show methane monooxigenase activity but it catalyzed H_2O_2 production. Miyaji *et al.* also reported the H_2O_2-producing activity of pMMO from *Methylosinus trichosporium* OB3b.[78] These data suggest that PmoB might be able to produce H_2O_2. The reactive oxygen species produced can catalyze the formation of methanol from methane. However, this interpretation should be carefully considered due to the presence of the H_2O_2 formation reactions mediated by duroquinol as discussed in the section 3.2 of this review.

3.8 Proposed catalytic mechanisms

According to the progress of the biochemical and biophysical analyses of pMMO, the proposed catalytic-site structures are changed from the trinuclear/dinuclear copper center to the mononuclear copper one.[53,71,96] Some catalytic mechanisms are proposed based on the predicted mononuclear copper site structures of pMMO, and the reactivity has been studied using computational methods. Yoshizawa and Shiota reported that the mononuclear copper Cu_A site is reactive to cleave the C–H bond of methane, in which Cu^{III}-oxo species is proposed as the active species for the reaction.[104] Morris reported the mechanism at the Cu_C site of pMMO, in which

the Cu^{III}-oxo species is proposed as the active site species.[105] Peng *et al.* also reported a catalytic mechanism using the Cu_C site with duroquinol as a part of the catalytic cycle. In this mechanism, the Cu^{II}–O anion-radical reacts with methane.[106] Thus, theoretical study supported the catalytic function of the mononuclear copper sites. Theoretical studies using the coordination of the Cu_{D1} site in the cryo-EM structure are expected.

Concluding remarks

The structure and function of the active sites of pMMO are still controversial. The main reason for this uncertainty is the unstable nature of pMMO. Despite extensive efforts to stabilize the enzyme, the specific activity remains very low and not highly reproducible. Although careful spectroscopic and structural work has been done, it is still unclear whether the data reflect the native enzyme, a damaged enzyme, or due to impurities and/or background. To further advance research in this field, it is essential to have access to highly active and stable enzyme samples as purified enzymes. Application of new methods like the one using bicelles and nanodiscs can contribute to further our understanding. A high-resolution structural model of the enzyme should be constructed from the highly active and stable enzyme samples using crystallography and/or cryo-EM methods. Spectroscopic analysis should be carefully performed based on the new structural models. It is also necessary to construct a heterologous and/or homologous expression system for this enzyme for mutational analysis of pMMO to identify the active site. Recently, cell-free biosynthesis of pMMO was reported, but it yielded an inactive enzyme.[107]

It is not feasible to use cells of methanotrophs or MMOs for the conversion of methane to methanol on an industrial scale due to difficulties with large-scale and high-cell-density cultivation of methanotrophs as well as with large-scale production of MMO proteins. It is also difficult to express MMOs in a fully or highly active form in heterologous hosts such as *E. coli*.[25,102] If MMOs can be heterologously expressed in methanol-utilizing bacteria and yeasts, such microbes could be used as a methane-oxidizing cell catalyst to directly produce useful compounds from methane. In these cells, methanol generated from methane can be rapidly metabolized and converted into useful compounds. The rapid consumption of methanol can also avoid product inhibition of MMOs by methanol.

Recently, we have succeeded in constructing methanol sensor cells in the methanol-utilizing yeast and bacterium in which the fluorescent proteins are expressed under the control of methanol-induced gene promoters.[108,109] Using the yeast methanol sensor, we have demonstrated that high-throughput screening of methanol-generating enzymes, *e.g.* pectin methylesterase, could be conducted.[108] Highly-functional novel methane-oxidizing biocatalysts will be developed by using these methanol sensor cells as expression hosts.

While the use of advanced technologies is expected, perhaps, we may need to go back to more basic research to identify stable enzymes by exploring new microorganisms. Considering the industrial importance of this enzyme, it is hoped that more researchers will enter this field and conduct active research.

Author contributions

Y. S., H. Y. and S. S. co-wrote the paper.

Conflicts of interest

The authors declare no conflicts of interest.

Acknowledgements

We thank Dr. Tomoyuki Takeya for his help in evaluation of non-enzymatic methane oxidation. This research work was supported by Japan Science and Technology Agency (CREST program JPMJCR to Y. S. and Mirai program JPMJMI22E8 to H. Y.) and Max Planck Society (S. S.). Open Access funding provided by the Max Planck Society.

References

1 R. Munõz, L. Meier, I. Diaz and D. Jeison, *Rev. Environ. Sci. Bio/Technol.*, 2015, **14**, 727–759.
2 B. Miao, S. S. K. Ma, X. Wang, H. B. Su and S. H. Chan, *Catal. Sci. Technol.*, 2016, **6**, 4048–4058.
3 A. Schoedel, Z. Ji and O. M. Yaghi, *Nat. Energy*, 2016, **1**, 16034.
4 M. J. da Silva, *Fuel Process. Technol.*, 2016, **145**, 42–61.
5 A. A. Latimer, A. Kakekhani, A. R. Kulkarni and J. K. Norskov, *ACS Catal.*, 2018, **8**, 6894–6907.
6 H. T. Luk, C. Mondelli, D. C. Ferre, J. A. Stewart and J. Perez-Ramirez, *Chem. Soc. Rev.*, 2017, **46**, 1358–1426.
7 R. S. Hanson and T. E. Hanson, *Microbiol. Rev.*, 1996, **60**, 439–471.
8 L. Chistoserdova, M. G. Kalyuzhnaya and M. E. Lidstrom, *Annu. Rev. Microbiol.*, 2009, **63**, 477–499.
9 R. Conrad, *Environ. Microbiol. Rep.*, 2009, **1**, 285–292.
10 C. Knief, *Curr. Issues Mol. Biol.*, 2019, **33**, 23–56.
11 S. Kirschke, P. Bousquet, P. Ciais, M. Saunois, J. G. Canadell, E. J. Dlugokencky, P. Bergamaschi, D. Bergmann, D. R. Blake, L. Bruhwiler, P. Cameron-Smith, S. Castaldi, F. Chevallier, L. Feng, A. Fraser, M. Heimann, E. L. Hodson, S. Houweling, B. Josse, P. J. Fraser, P. B. Krummel, J. F. Lamarque, R. L. Langenfelds, C. Le Quere, V. Naik, S. O'Doherty, P. I. Palmer, I. Pison, D. Plummer, B. Poulter, R. G. Prinn, M. Rigby, B. Ringeval, M. Santini, M. Schmidt, D. T. Shindell, I. J. Simpson, R. Spahni, L. P. Steele, S. A. Strode, K. Sudo, S. Szopa, G. R. van der Werf, A. Voulgarakis, M. van Weele, R. F. Weiss, J. E. Williams and G. Zeng, *Nat. Geosci.*, 2013, **6**, 813–823.
12 M. Saunois, P. Bousquet, B. Poulter, A. Peregon, P. Ciais, J. G. Canadell, E. J. Dlugokencky, G. Etiope, D. Bastviken, S. Houweling, G. Janssens-Maenhout, F. N. Tubiello, S.

Castaldi, R. B. Jackson, M. Alexe, V. K. Arora, D. J. Beerling, P. Bergamaschi, D. R. Blake, G. Brailsford, V. Brovkin, L. Bruhwiler, C. Crevoisier, P. Crill, K. Covey, C. Curry, C. Frankenberg, N. Gedney, L. Hoglund-Isaksson, M. Ishizawa, A. Ito, F. Joos, H. S. Kim, T. Kleinen, P. Krummel, J. F. Lamarque, R. Langenfelds, R. Locatelli, T. Machida, S. Maksyutov, K. C. McDonald, J. Marshall, J. R. Melton, I. Morino, V. Naik, S. O'Doherty, F. J. W. Parmentier, P. K. Patra, C. H. Peng, S. S. Peng, G. P. Peters, I. Pison, C. Prigent, R. Prinn, M. Ramonet, W. J. Riley, M. Saito, M. Santini, R. Schroeder, I. J. Simpson, R. Spahni, P. Steele, A. Takizawa, B. F. Thornton, H. Q. Tian, Y. Tohjima, N. Viovy, A. Voulgarakis, M. van Weele, G. R. van der Werf, R. Weiss, C. Wiedinmyer, D. J. Wilton, A. Wiltshire, D. Worthy, D. Wunch, X. Y. Xu, Y. Yoshida, B. Zhang, Z. Zhang and Q. Zhu, *Earth Syst. Sci. Data*, 2016, **8**, 697–751.

13 F. Keppler, J. T. G. Hamilton, M. Brass and T. Rockmann, *Nature*, 2006, **439**, 187–191.

14 L. Ernst, B. Steinfeld, U. Barayeu, T. Klintzsch, M. Kurth, D. Grimm, T. P. Dick, J. G. Rebelein, I. B. Bischofs and F. Keppler, *Nature*, 2022, **603**, 482–487.

15 J. D. Semrau, A. A. DiSpirito, W. Y. Gu and S. Yoon, *Appl. Environ. Microbiol.*, 2018, **84**, e02289-17.

16 C. W. Koo and A. C. Rosenzweig, *Chem. Soc. Rev.*, 2021, **50**, 3424–3436.

17 S. I. Chan, V. C. C. Wang, P. P. Y. Chen and S. S. F. Yu, *J. Chin. Chem. Soc.*, 2022, **69**, 1147–1158.

18 R. Banerjee, J. C. Jones and J. D. Lipscomb, *Annu. Rev. Biochem.*, 2019, **88**, 409–431.

19 W. X. Wang, A. D. Liang and S. J. Lippard, *Acc. Chem. Res.*, 2015, **48**, 2632–2639.

20 M. R. Hyman, I. B. Murton and D. J. Arp, *Appl. Environ. Microbiol.*, 1988, **54**, 3187–3190.

21 K. H. Halsey, L. A. Sayavedra-Soto, P. J. Bottomley and D. J. Arp, *J. Bacteriol.*, 2006, **188**, 4962–4969.

22 I. Y. Hwang, S. H. Lee, Y. S. Choi, S. J. Park, J. G. Na, I. S. Chang, C. Kim, H. C. Kim, Y. H. Kim, J. W. Lee and E. Y. Lee, *J. Microbiol. Biotechnol.*, 2014, **24**, 1597–1605.

23 M. M. Cui, A. Z. Ma, H. Y. Qi, X. L. Zhuang and G. Q. Zhuang, *Microbiology*, 2015, **4**, 1–11.

24 W. T. Yang, L. D. Shen and Y. N. Bai, *Environ. Res.*, 2023, **219**, 115174.

25 M. O. Ross and A. C. Rosenzweig, *J. Biol. Inorg. Chem.*, 2017, **22**, 307–319.

26 J. D. Semrau, A. A. DiSpirito and S. Yoon, *FEMS Microbiol. Rev.*, 2010, **34**, 496–531.

27 Y. Hibi, K. Asai, H. Arafuka, M. Hamajima, T. Iwama and K. Kawai, *J. Biosci. Bioeng.*, 2011, **111**, 547–549.

28 T. Nakagawa, R. Mitsui, A. Tani, K. Sasa, S. Tashiro, T. Iwama, T. Hayakawa and K. Kawai, *PLoS One*, 2012, **7**, e50480.

29 L. Chistoserdova and M. G. Kalyuzhnaya, *Trends Microbiol.*, 2018, **26**, 703–714.

30 M. C. F. van Teeseling, A. Pol, H. R. Harhangi, S. van der Zwart, M. S. M. Jetten and H. J. M. O. den Camp, *Appl. Environ. Microbiol.*, 2014, **80**, 6782–6791.

31 A. F. Khadem, A. Pol, A. Wieczorek, S. S. Mohammadi, K. J. Francoijs, H. G. Stunnenberg, M. S. M. Jetten and H. J. M. Op den Camp, *J. Bacteriol.*, 2011, **193**, 4438–4446.

32 M. F. Ul Haque, H. J. Xu, J. C. Murrell and A. Crombie, *Microbiology*, 2020, **166**, 894–908.

33 S. Guerrero-Cruz, A. Vaksmaa, M. A. Horn, H. Niemann, M. Pijuan and A. Ho, *Front. Microbiol.*, 2021, **12**, 678057.

34 H. J. M. Op den Camp, T. Islam, M. B. Stott, H. R. Harhangi, A. Hynes, S. Schouten, M. S. M. Jetten, N. K. Birkeland, A. Pol and P. F. Dunfield, *Environ. Microbiol. Rep.*, 2009, **1**, 293–306.

35 R. J. M. Van Spanning, Q. Guan, C. Melkonian, J. Gallant, L. Polerecky, J. F. Flot, B. W. Brandt, M. Braster, P. I. Espinoza, J. W. Aerts, M. M. Meima-Franke, S. R. Piersma, C. M. Bunduc, R. Ummels, A. Pain, E. J. Fleming, N. N. Van der Wel, V. D. Gherman, S. M. Sarbu, P. L. E. Bodelier and W. Bitter, *Nat. Microbiol.*, 2022, **7**, 2089–2100.

36 J. C. Murrell, B. Gilbert and I. R. McDonald, *Arch. Microbiol.*, 2000, **173**, 325–332.

37 R. L. Lieberman and A. C. Rosenzweig, *Nature*, 2005, **434**, 177–182.

38 A. El Ghazouani, A. Basle, S. J. Firbank, C. W. Knapp, J. Gray, D. W. Graham and C. Dennison, *Inorg. Chem.*, 2011, **50**, 1378–1391.

39 C. S. Kang-Yun, X. J. Liang, P. Dershwitz, W. Y. Gu, A. Schepers, A. Flatley, J. Lichtmannegger, H. Zischka, L. J. Zhang, X. Lu, B. H. Gu, J. C. Ledesma, D. J. Pelger, A. A. DiSpirito and J. D. Semrau, *ISME J.*, 2022, **16**, 211–220.

40 R. Banerjee, Y. Proshlyakov, J. D. Lipscomb and D. A. Proshlyakov, *Nature*, 2015, **518**, 431–434.

41 G. P. Stafford, J. Scanlan, I. R. McDonald and J. C. Murrell, *Microbiology*, 2003, **149**, 1771–1784.

42 J. D. Semrau, S. Jagadevan, A. A. DiSpirito, A. Khalifa, J. Scanlan, B. H. Bergman, B. C. Freemeier, B. S. Baral, N. L. Bandow, A. Vorobev, D. H. Haft, S. Vuilleumier and J. C. Murrell, *Environ. Microbiol.*, 2013, **15**, 3077–3086.

43 J. G. Leahy, P. J. Batchelor and S. M. Morcomb, *FEMS Microbiol. Rev.*, 2003, **27**, 449–479.

44 N. V. Coleman, N. B. Bui and A. J. Holmes, *Environ. Microbiol.*, 2006, **8**, 1228–1239.

45 A. T. Crombie and J. C. Murrell, *Nature*, 2014, **510**, 148–151.

46 C. E. Tinberg and S. J. Lippard, *Acc. Chem. Res.*, 2011, **44**, 280–288.

47 Y. A. Zhu, C. W. Koo, C. K. Cassidy, M. C. Spink, T. Ni, L. C. Zanetti-Domingues, B. Bateman, M. L. Martin-Fernandez, J. Shen, Y. W. Sheng, Y. Song, Z. Y. Yang, A. C. Rosenzweig and P. J. Zhang, *Nat. Commun.*, 2022, **13**, 5221.

48 S. S. F. Yu, K. H. C. Chen, M. Y. H. Tseng, Y. S. Wang, C. F. Tseng, Y. J. Chen, D. S. Huang and S. I. Chan, *J. Bacteriol.*, 2003, **185**, 5915–5924.

49 H. H. T. Nguyen, A. K. Shiemke, S. J. Jacobs, B. J. Hales, M. E. Lidstrom and S. I. Chan, *J. Biol. Chem.*, 1994, **269**, 14995–15005.

50 D. Drummond, S. Smith and H. Dalton, *Eur. J. Biochem.*, 1989, **182**, 667–671.

51 S. Y. Ro, M. O. Ross, Y. W. Deng, S. Batelu, T. J. Lawton, J. D. Hurley, T. L. Stemmler, B. M. Hoffman and A. C. Rosenzweig, *J. Biol. Chem.*, 2018, **293**, 10457–10465.
52 S. Y. Ro, L. F. Schachner, C. W. Koo, R. Purohit, J. P. Remis, G. E. Kenney, B. W. Liauw, P. M. Thomas, S. M. Patrie, N. L. Kelleher and A. C. Rosenzweig, *Nat. Commun.*, 2019, **10**, 2675.
53 C. W. Koo, F. J. Tucci, Y. He and A. C. Rosenzweig, *Science*, 2022, **375**, 1287–1291.
54 H. H. T. Nguyen, S. J. Elliott, J. H. K. Yip and S. I. Chan, *J. Biol. Chem.*, 1998, **273**, 7957–7966.
55 J. A. Zahn and A. A. DiSpirito, *J. Bacteriol.*, 1996, **178**, 1018–1029.
56 A. Miyaji, T. Kamachi and I. Okura, *Biotechnol. Lett.*, 2002, **24**, 1883–1887.
57 M. Takeguchi, K. Miyakawa and I. Okura, *J. Mol. Catal. A: Chem.*, 1998, **132**, 145–153.
58 R. L. Lieberman, D. B. Shrestha, P. E. Doan, B. M. Hoffman, T. L. Stemmler and A. C. Rosenzweig, *Proc. Natl. Acad. Sci. U. S. A.*, 2003, **100**, 3820–3825.
59 G. M. Tonge, D. E. F. Harrison and I. J. Higgins, *Biochem. J.*, 1977, **161**, 333–344.
60 R. I. Gvozdev, I. A. Tukhvatullin and L. V. Tumanova, *Biol. Bull.*, 2008, **35**, 161–169.
61 M. Takeguchi, K. Miyakawa and I. Okura, *J. Mol. Catal. A: Chem.*, 1999, **137**, 161–168.
62 A. Miyaji, M. Nitta and T. Baba, *J. Biotechnol.*, 2019, **306S**, 100001.
63 M. Takeguchi and I. Okura, *Catal. Surv. Jpn.*, 2000, **4**, 51–63.
64 S. A. Cook and A. K. Shiemke, *J. Inorg. Biochem.*, 1996, **63**, 273–284.
65 J. D. Semrau, D. Zolandz, M. E. Lidstrom and S. I. Chan, *J. Inorg. Biochem.*, 1995, **58**, 235–244.
66 K. J. Burrows, A. Cornish, D. Scott and I. J. Higgins, *J. Gen. Microbiol.*, 1984, **130**, 3327–3333.
67 D. W. Choi, R. C. Kunz, E. S. Boyd, J. D. Semrau, W. E. Antholine, J. I. Han, J. A. Zahn, J. M. Boyd, A. M. de la Mora and A. A. DiSpirito, *J. Bacteriol.*, 2003, **185**, 5755–5764.
68 A. K. Shiemke, S. A. Cook, T. Miley and P. Singleton, *Arch. Biochem. Biophys.*, 1995, **321**, 421–428.
69 I. M. Ibrahim, H. Wu, R. Ezhov, G. E. Kayanja, S. D. Zakharov, Y. Y. Du, W. A. Tao, Y. Pushkar, W. A. Cramer and S. Puthiyaveetil, *Commun. Biol.*, 2020, **3**, 13.
70 E. Cadenas, A. Boveris, C. I. Ragan and A. O. M. Stoppani, *Arch. Biochem. Biophys.*, 1977, **180**, 248–257.
71 M. O. Ross, F. MacMillan, J. Z. Wang, A. Nisthal, T. J. Lawton, B. D. Olafson, S. L. Mayo, A. C. Rosenzweig and B. M. Hoffman, *Science*, 2019, **364**, 566–570.
72 M. R. Gunther, P. M. Hanna, R. P. Mason and M. S. Cohen, *Arch. Biochem. Biophys.*, 1995, **316**, 515–522.
73 B. Halliwell and J. M. C. Gutteridge, *Biochem. J.*, 1984, **219**, 1–14.
74 M. D. Pham, Y. P. Lin, Q. V. Vuong, P. Nagababu, B. T. A. Chang, K. Y. Ng, C. H. Chen, C. C. Han, C. H. Chen, M. S. Li, S. S. F. Yu and S. I. Chan, *Biochim. Biophys. Acta*, 2015, **1854**, 1842–1852.
75 S. D. Prior and H. Dalton, *FEMS Microbiol. Lett.*, 1985, **29**, 105–109.
76 V. I. Vasil'ev, T. V. Tikhonova, R. I. Gvozdev, I. A. Tukhvatullin and V. O. Popov, *Biochemistry*, 2006, **71**, 1329–1335.
77 K. H. C. Chen, H. H. Wu, S. F. Ke, Y. T. Rao, C. M. Tu, Y. P. Chen, K. H. Kuei, Y. S. Chen, V. C. C. Wang, W. C. Kao and S. I. Chan, *J. Inorg. Biochem.*, 2012, **111**, 10–17.
78 A. Miyaji, M. Suzuki, T. Baba, T. Kamachi and I. Okura, *J. Mol. Catal. B: Enzym.*, 2009, **57**, 211–215.
79 S. M. Smith, S. Rawat, J. Telser, B. M. Hoffman, T. L. Stemmler and A. C. Rosenzweig, *Biochemistry*, 2011, **50**, 10231–10240.
80 S. Sirajuddin, D. Barupala, S. Helling, K. Marcus, T. L. Stemmler and A. C. Rosenzweig, *J. Biol. Chem.*, 2014, **289**, 21782–21794.
81 A. S. Hakemian, K. C. Kondapalli, J. Telser, B. M. Hoffman, T. L. Stemmler and A. C. Rosenzweig, *Biochemistry*, 2008, **47**, 6793–6801.
82 W. H. Chang, H. H. Lin, I. K. Tsai, S. H. Huang, S. C. Chung, I. P. Tu, S. S. F. Yu and S. I. Chan, *J. Am. Chem. Soc.*, 2021, **143**, 9922–9932.
83 P. P. Y. Chen and S. I. Chan, *J. Inorg. Biochem.*, 2006, **100**, 801–809.
84 C. H. Yeh, S. S. F. Yu, S. I. Chan and J. C. Jiang, *ChemistrySelect*, 2018, **3**, 5113–5122.
85 S. I. Chan, V. C. C. Wang, J. C. H. Lai, S. S. F. Yu, P. P. Y. Chen, K. H. C. Chen, C. L. Chen and M. K. Chan, *Angew. Chem., Int. Ed.*, 2007, **46**, 1992–1994.
86 S. Maji, J. C. M. Lee, Y. J. Lu, C. L. Chen, M. C. Hung, P. P. Y. Chen, S. S. F. Yu and S. I. Chan, *Chem. – Eur. J.*, 2012, **18**, 3955–3968.
87 P. Nagababu, S. Maji, M. P. Kumar, P. P. Y. Chen, S. S. F. Yu and S. I. Chan, *Adv. Synth. Catal.*, 2012, **354**, 3275–3282.
88 S. I. Chan, C. Y. C. Chien, C. S. C. Yu, P. Nagababu, S. Maji and P. P. Y. Chen, *J. Catal.*, 2012, **293**, 186–194.
89 Y. H. Chen, C. Q. Wu, P. H. Sung, S. I. Chan and P. P. Y. Chen, *ChemCatChem*, 2020, **12**, 3088–3096.
90 P. P. Y. Chen, R. B. G. Yang, J. C. M. Lee and S. I. Chan, *Proc. Natl. Acad. Sci. U. S. A.*, 2007, **104**, 14570–14575.
91 R. L. Lieberman and A. C. Rosenzweig, *Crit. Rev. Biochem. Mol. Biol.*, 2004, **39**, 147–164.
92 R. L. Lieberman, K. C. Kondapalli, D. B. Shrestha, A. S. Hakemian, S. M. Smith, J. Telser, J. Kuzelka, R. Gupta, A. S. Borovik, S. J. Lippard, B. M. Hoffman, A. C. Rosenzweig and T. L. Stemmler, *Inorg. Chem.*, 2006, **45**, 8372–8381.
93 H. Yuan, M. L. P. Collins and W. E. Antholine, *J. Am. Chem. Soc.*, 1997, **119**, 5073–5074.
94 H. Yuan, M. L. P. Collins and W. E. Antholine, *Biophys. J.*, 1999, **76**, 2223–2229.
95 L. L. Cao, O. Caldararu, A. C. Rosenzweig and U. Ryde, *Angew. Chem., Int. Ed.*, 2018, **57**, 162–166.
96 R. J. Jodts, M. O. Ross, C. W. Koo, P. E. Doan, A. C. Rosenzweig and B. M. Hoffman, *J. Am. Chem. Soc.*, 2021, **143**, 15358–15368.
97 E. F. Liew, D. C. Tong, N. V. Coleman and A. J. Holmes, *Microbiology*, 2014, **160**, 1267–1277.

98 G. E. Cutsail, M. O. Ross, A. C. Rosenzweig and S. DeBeer, *Chem. Sci.*, 2021, **12**, 6194–6209.
99 R. Balasubramanian, S. M. Smith, S. Rawat, L. A. Yatsunyk, T. L. Stemmler and A. C. Rosenzweig, *Nature*, 2010, **465**, 115–119.
100 M. A. Culpepper, G. E. Cutsail, B. M. Hoffman and A. C. Rosenzweig, *J. Am. Chem. Soc.*, 2012, **134**, 7640–7643.
101 M. A. Culpepper, G. E. Cutsail, W. A. Gunderson, B. M. Hoffman and A. C. Rosenzweig, *J. Am. Chem. Soc.*, 2014, **136**, 11767–11775.
102 H. J. Kim, J. Huh, Y. W. Kwon, D. Park, Y. Yu, Y. E. Jang, B. R. Lee, E. Jo, E. J. Lee, Y. Heo, W. Lee and J. Lee, *Nat. Catal.*, 2019, **2**, 342–353.
103 Y. J. Lu, M. C. Hung, B. T. A. Chang, T. L. Lee, Z. H. Lin, I. K. Tsai, Y. S. Chen, C. S. Chang, Y. F. Tsai, K. H. C. Chen, S. I. Chan and S. S. F. Yu, *J. Inorg. Biochem.*, 2019, **196**, 110691.
104 K. Yoshizawa and Y. Shiota, *J. Am. Chem. Soc.*, 2006, **128**, 9873–9881.
105 R. H. Morris, *Inorg. Chim. Acta*, 2020, **503**, 119441.
106 W. Peng, X. Y. Qu, S. Shaik and B. J. Wang, *Nat. Catal.*, 2021, **4**, 266–273.
107 C. W. Koo, J. M. Hershewe, M. C. Jewett and A. C. Rosenzweig, *ACS Synth. Biol.*, 2022, **11**, 4009–4017.
108 T. Takeya, H. Yurimoto and Y. Sakai, *Appl. Microbiol. Biotechnol.*, 2018, **102**, 7017–7027.
109 V. C. Casaroli, I. Orita, S. Katayama, H. Yurimoto, Y. Sakai and T. Fukui, *J. Biosci. Bioeng.*, 2021, **132**, 247–252.

